

1 Referee #2

2 We thank you for your careful reading of the manuscript, helpful comments and suggestions. We
3 have made revisions according to your comments and suggestions in view of a positive
4 reconsideration of the manuscript for publication.

5

6 **In this study MSG images are used for the early detection and monitoring of the**
7 **evolution of storm cells associated with MCSs. In particular, Airmass and Convection**
8 **RGB composites are used at 15 minute time interval and applied to one case study (19-**
9 **22 February 2013) when a depression developed over Africa and moved across the**
10 **Mediterranean resulting in deep convection along its trajectory and in an extreme**
11 **weather event in the Attica region in Greece. The article is reasonably well written and**
12 **the topic fits well with the scope of the journal. However, as it stands now, it offers a**
13 **minimal contribution to the existing knowledge of the use of MSG SEVIRI data (in**
14 **particular RGB composites) for detection and monitoring of severe convection. It is**
15 **worth noting that the use of RGB composites at 15 minute time interval has become a**
16 **widely used techniques for severe weather monitoring and operational nowcasting in**
17 **different national and regional weather service agencies throughout Europe. These**
18 **composites have been available, documented and used for several years now. On the**
19 **EUMETSAT web site <http://oiswww.eumetsat.org/IPPS/html/MSG/RGB/> there is a full**
20 **description of how they are produced and how to interpret them and several**
21 **applications and case studies are described (see also www.eumetrain.org). Moreover, an**
22 **"assessment" (referred to in the title) should be based on a significant number of case**
23 **studies, while the paper is about the application of widely used MSG RGB composites to**
24 **one case study only. In conclusion, in my opinion the paper is not suitable for**
25 **publication.**

26 The purpose of the paper was not to demonstrate the potential of RGB composites; we fully
27 agree with your comment, namely that their potential has been well documented by
28 EUMETSAT and other case studies. In practice we wanted to examine an extreme weather
29 event in the Attica region in Greece through the use of composites, synoptic maps, ground
30 based data, etc. This event did cause considerable damages in Athens and SE Greece and
31 raised great attention in the scientific community (in Greece) which is involved in disaster and
32 risk management, the public as well the public authorities on the potential of satellites to
33 detect, monitor and assess mesoscale convection systems and/or extreme weather events as

1 well as in supporting nowcasting (RGB composites are not used by the Greek National
2 Meteorological Service). The attention was further enhanced by the fact that the MCSs were
3 dissipated and reinforced due to the supply of warm and moist air from the southern part of
4 the Mediterranean.

5 Finally the comment that the word “assessment” is not appropriate for the title of this paper
6 (as only one case study was examined) is correct. What we meant to say was rather
7 “examination” than “assessment”, thus the title has been changed to "Detection and
8 monitoring of storm cells associated with natural hazards -an application to an extreme
9 weather event over Athens - Greece".

10

11

12 • Specific Comments

13

14 **At the end of Section 3 the authors state: "In this study, improvements of the algorithms refer to**
15 **(a) the estimation of the solar zenith angle per pixel, thus enabling the processing of MSG data,**
16 **and (b) the production of the composites every 15 min". Besides the claimed use of the solar zenith**
17 **angle correction (which should be described in detail), I do not see a new methodology developed.**

18 The word “improvement” is not appropriate. We meant that we calculated the solar zenith
19 angle, which is basic, and it is not included in the Metadata of the satellite images. The
20 production of composites every 15 minutes is not an improvement of the algorithm but rather
21 an improvement of the temporal frequency of acquired information in terms of the
22 composites. A respective clarification has been made in the text.

23

24 **It is well known that Airmass composite depicts well the synoptic situation and detects the PV**
25 **anomaly prior to the depression development. In the present study the product is used also for**
26 **storm cell detection (on 22 February). In Fig. 11 the Airmass RGB composite is shown at four**
27 **specific times, and related to the precipitation maxima registered at three weather stations (Fig.**
28 **12). However, it is not clear why precisely these four images have been selected. There is no**
29 **indication of the criteria used to establish that these four images have MCSs developed. What are**
30 **the features of MCS's that are evident in these four images and that are not evident in all the other**
31 **images in that time frame?**

32

33 The MCSs were developed over extensive cloudiness and consequently they are not very distinct. The
34 criteria used apart from the brightness temperature that is not shown, were the geometrical
35 characteristics. As it can be seen in the **revised** Figure 11b (now Figure 10b), where the weather
36 stations are also depicted, the first MCS appears larger with oval shape.

37

1 **How are the Convective storm composite images shown in Fig. 9 related to precipitation records?**
2 **Geographical coordinates (Lat Lon) should be provided for all images, or evidence Attica region in**
3 **some way (in Particular Fig. 6, 9, 11). It might be useful to indicate the position of the weather**
4 **station (used as reference for precipitation amounts) in Fig. 11.**

5

6 We added the weather station positions in Figures 9 and 11 (now Figure 8 and 10) and not borders
7 for better visual interpretation. We made the border lines red in the Figure 6 (now Figure 5).

8

9

"Detection and monitoring of storm cells associated with natural hazards -an application to an extreme weather event over Athens - Greece"

Thaleia Mavroukou^{1*}, Constantinos Cartalis¹

[1]Division of Physics, Department of Environmental Physics, University of Athens, 15874 Athens, Greece

Correspondence to: T. Mavroukou (thmavroukou@phys.uoa.gr)

Abstract

Storm cells that evolve in Mesoscale Convective Systems (MCSs) can be recognised with the use of satellite images. In this study, Meteosat images are used for the early detection and monitoring of the evolution of storm cells associated with MCSs. The developed methodology is based on the estimation of the "Airmass" and "Convective storm" composites, at fifteen minutes intervals. The methodology was applied on a selected four - day case study in February 2013, when a depression was developed over Africa and moved across the Mediterranean resulting in deep convection along its trajectory and in an extreme weather event (heavy rainfall associated with severe flooding) at the wider urban agglomeration of Athens. The produced composites detect potential vorticity (PV) anomaly related to cyclogenesis and increase the potential to detect and monitor storm cells associated with natural hazards.

1 Introduction

Satellite remote sensing may effectively detect and monitor Mesoscale Convective Systems (MCSs) thus as well as support the nowcasting of convective systems.

A Mesoscale Convective System (MCS) accounts for the occurrence of severe storm causing flooding and destructions (Houze 2004). A MCS is a convective cloud and precipitation system quite larger than an individual storm and is characterized by extensive cloudiness in the middle and upper troposphere for hundred kilometres in the horizontal dimension (Glickman 2000). It is developed from individual cells that interact with each other, merge

1 and subsequently form a well-organized, long lived convective system (Cotton and & Anthes
2 1989). Houze (2004) points out that the dynamical processes of a MCSs are often more
3 complex than those of individual cumulonimbus clouds, because when these clouds group
4 together additional phenomena appear, like mesoscale circulations.

5 According to a number of studies (Maddox 1983; Cotton and Anthes et al. 1989; Anderson
6 and Arritt 1998; Laing and Fritsch 2000), the causes for the development of MCSs are:

- 7 • Existence of warm advection in the lower troposphere; the associated convection
8 contributes to the development and the maintenance of an MCS.
- 9 • Existence of strong south wind (low-level jet) with subsequent transfer of warm and
10 moist air in the region of the MCS development.
- 11 • Strong divergence in the region resulting in the enhancement of convection.
- 12 • Convergence at the surface, often due to the existence of frontal surface

13 In addition it was found that MCSs usually develop at the right entrance or left exit of jet
14 stream.

15 Many researchers have attempted to predict and analyse deep convection, thus possible MCS
16 development (Pankiewicz 1997, Vila and Machado 2004, Kolios and Feidas 2010). Melani et
17 al. (2013) highlights the key role of the Mediterranean Sea in the development of the MCSs
18 and points out the significance of the mechanism of convective initiation for the forecasting
19 improvement. Furthermore, Pajek et al. (2007) indicate that “the process of storm
20 development consists of pre-storm conditions leading to the development of convection
21 followed by development of deep convective clouds, which became storm cells after the first
22 lightning”; they also concluded that the use of satellite data at specific spectral channels may
23 increase lead –time for storm nowcasting.

24 Pre-storm conditions are characterized by instability in the atmosphere which results in deep
25 convection and consequently to the development of storm cells (Pajek et al 2007).
26 Atmospheric instability during winter, over southeast Europe, is generated when cold
27 continental air mass encounters a warmer Mediterranean one. Evaporation that takes place
28 over the relative warm Mediterranean and Greek maritime areas enforces this instability,
29 while during the cold period of the year Greece is affected mainly by westward depressions
30 formed over the Mediterranean (Cartalis et al. 2004). According to some authors (Petterssen,
31 1956; Radinovic, 1987; Campins et al. 2000) the Mediterranean region is one of the most

1 cyclogenetic regions in the world, while the Mediterranean cyclone structure can be well
2 described with the use of the midlatitude conveyor belt model (Ziv et al., 2010) and the
3 cyclogenetic mechanism has been well explained through the potential vorticity (PV)
4 dynamics (Hoskins et al. 1985; Davis and Emanuel 1991). Therefore, black lines in the water
5 vapour satellite images are associated with the inflow of dry stratospheric air and
6 consequently could serve as indicators of imminent cyclogenetic events (Michel and
7 Bouttier, 2006). An example of a Meteosat water vapour image depicting dry air intrusion in a
8 Mediterranean cyclone is illustrated in a study regarding the relation of midlatitude conveyor
9 belts to winter Mediterranean cyclones (Ziv et al., 2010).

10 Regarding the eastern Mediterranean and specifically Greece, Feidas et al. (2000) developed a
11 cloud classification scheme of satellite images in the visible, infrared and water vapour
12 channels aiming to define and monitor heavy rain associated cloud cells. Feidas and Cartalis
13 (2001) developed an automated algorithm, capable of locating regions that are characterized
14 by deep convection and consequently of detecting and monitoring MCSs until the point of
15 dissipation. The algorithm was applied to events characterized by heavy rainfall in Greece; it
16 detected several MCSs on infrared and water vapour satellite images (Feidas and Cartalis
17 2001; Feidas and Cartalis 2005). However, the above techniques employed Meteosat First
18 Generation (MFG) satellite data of lower temporal, spatial and spectral resolutions as
19 compared to Meteosat Second Generation (MSG).

20 The MSG satellite provides data which, apart from the better spatial and temporal resolutions,
21 is of improved spectral resolution thus enabling the application of multispectral techniques in
22 many fields such as surface observations, fire and cloud detection, etc. (Casanova et al 2010).
23 Giannakos and Feidas (2013) used brightness temperature differences as spectral parameters,
24 along with textural differences as derived from the infrared MSG channel, in order to classify
25 stratiform and convective rain. In addition, the technique described by Negri et al (2014)
26 assumes that combinations of infrared pairs of the SEVIRI channel allow the isolation of
27 specific cloud components (droplets or ice particles with different shape and size) and then
28 the tracking of the displacement of these structures, so as to detect deep convection cloud-
29 tops.

30 Furthermore, composites enable the visualisation of multispectral physical features in a single
31 image, such as pre-storm conditions and storm cell characteristics. The MSG composites
32 proposed by Kerkmann. et al. (2006) have been used in studies for the detection and analysis

1 of MCSs in Europe (Pajek et al. 2007, Feidas 2012). In an operational approach towards the
2 nowcasting of an MCS development in southwest Italy, Gallino and Turato (2006) presented
3 the importance of the 6.2 μm spectral channel as it depicts in detail the conditions in the upper
4 troposphere which have an important role in the development of the MCSs. At the same time
5 they suggested the use of the Convective storm composite in MCS detection so as to support
6 the the distinction of young and severe storms in daytime. Among other differences this
7 composite employs the 3.9 μm - 10.8 μm channel difference resulting in the depiction of
8 small ice particles, which reflects a feature of deep convection and severe weather. In another
9 study, regarding two MCSs that crossed Hungary in 2006, Putsay et al. (2009) used the
10 Airmass composite for the interpretation of the synoptic conditions during day and night. This
11 composite allows the distinction of different air masses, of the cloudiness linked with frontal
12 surfaces and of the jet stream, i.e. factors that affect instability and consequently the
13 development of a MCS.

14 In this study the composites were reproduced and applied for an extreme weather event which
15 occurred in the region of Athens in February 2013. All composites are produced at fifteen
16 minutes intervals in an effort to track MCSs from the time of genesis until the time of
17 dissipation. The potential of the composites to support operational nowcasting is examined, in
18 relation also to ground based measurements of precipitation.

19 **2 Data**

20 The area of study is provided in Fig. 1 in Meteosat projection; it covers Central Europe and
21 the Eastern Mediterranean (59°04 00' N, 06°97 00' W, 28°23 00' N, 30°00 00' E). The study is
22 further concentrated to the Attica region and the wider urban agglomeration of Athens.

23 Meteosat 8 images, for five infrared and two visible channels, were obtained for the period
24 19-22 February, 2013. The Airmass and Convective storm composites were produced at
25 fifteen minute intervals using the channels shown in Table 1. In addition, synoptic data from
26 the European Centre of Medium-Range Forecasts (ECMWF) as well as from Eumetrain, were
27 used covering the same area and time period, in order to verify the results as well as to
28 support their analysis. Precipitation data, at ten minutes intervals, were collected from eight
29 stations (network of the National and Technical University of Athens) within the Attica
30 region (Fig. 2).

1 **3 Methodology**

2 The methodology for the early detection of storm cells consists of the following steps:

- 3 • Production of the Airmass and the Convective storm composites production according
4 to Kerkmann. et al. (2006); the Airmass and Convective storm composites are considered
5 appropriate for the depiction of the pre-storm conditions and the analysis of the associated
6 severe weather, whereas their combination allows the continuous monitoring of their
7 evolution in time;
- 8 • Application of the composites for a case study reflecting an extreme weather event.
- 9 • Evaluate the potential of the methodology for the detection of MCS and the
10 subsequent improvement of operational nowcasting.

11 The Airmass composite provides data in day and night as it consists of two water vapour
12 channels with centre wavelengths at 6.2 (WV6.2) and 7.3 μm (WV7.3) and two infrared
13 channels with centre wavelengths at 9.7 (IR9.7) and 10.8 μm (IR10.8) in the following
14 combination:

$$15 \quad \text{RED} = \text{WV6.2} - \text{WV 7.3}$$

$$16 \quad \text{GREEN} = \text{IR9.7} - \text{IR10.8}$$

$$17 \quad \text{BLUE} = \text{WV6.2}$$

18 The Convective storm composite provides data in daytime only as it consists of four infrared
19 channels with wavelengths at 6.2 (WV6.2), 7.3 (WV7.3), 3.9 (IR3.9), 10.8 μm (IR10.8) and
20 one visible channel with wavelengths at 0.6 (VIS0.6) and one in the near infrared at 1.6 μm
21 (NIR1,6) in the following combination:

$$22 \quad \text{RED} = \text{WV6.2-WV7.3}$$

$$23 \quad \text{GREEN} = \text{IR3.9-IR10.8}$$

$$24 \quad \text{BLUE} = \text{NIR1.6-VIS0.6}$$

25 The Airmass composite was selected in order to define potential instability in the atmosphere
26 (and in particular to monitor synoptic conditions, upper level dynamics and different air
27 masses). The Convective storm composite was selected so as to monitor the convection
28 related to storm development, i.e. strong updrafts as depicted through the detection of small
29 ice particles in the upper troposphere.

1 During night time, and due to lack of data in the visible bands, the Convective storm
2 composite is not applicable and the use of Airmass composite is extended for the detection of
3 storm cells. This is accomplished by adapting the traditional approach of storm cell detection
4 in the Airmass composite interpretation. According to Feidas and Cartalis (2001), a storm cell
5 is defined as a cloud system with low brightness temperature in the IR channels with specific
6 geometrical characteristics (circular).

7 **3.1 Processing the satellite data**

8 The procedure followed for the production of the Airmass and the Convective storm
9 composites is analysed below while the overall procedure for both composites is presented
10 also as a flow chart in Fig. 3 and Fig. 4 respectively.

11 The procedure for the Airmass composite (Figure 3) consists of the conversion of the pixel
12 values to brightness temperature, the calculation of the brightness temperature differences and
13 the application of linear stretch and colour to the resulted differences. The difference in the
14 red channel provides information about the altitude of a humid layer or cloud as the two WV
15 channels detect humidity in different altitudes. The difference in green provides information
16 about the ozone concentration in the atmosphere and consequently about the height of the
17 tropopause, the existence of warm or cold air masses and the intrusion of ozone-rich
18 stratospheric air. Furthermore, in blue the WV6.2 channel is assigned, giving information on
19 the existence of humidity or cloudiness in the layer 500-200 hPa. In the Airmass image, the
20 above physical features are preserved through the assignment of the scale in the Brightness
21 Temperature Differences (BTD) values. Green colours indicate warm air masses, while blue
22 shades indicate cold air masses. White colour corresponds to height precipitating clouds while
23 whiter and brighter colours indicate high altitude clouds and consequently low temperatures.
24 Red colours indicate sinking dry air, which could be of stratospheric origin and consequently
25 enabling monitoring the jet stream.

26 The procedure followed for the Convective storm composite production (Figure 4) regarding
27 the infrared data is similar to the Airmass one. Additionally, this procedure requires
28 calculations of the BT 3.9 CO₂ correction, as this channel lies close to the CO₂ absorption
29 band, and of the solar zenith angle per pixel. It should be mentioned that the latter is essential
30 for the calculation of reflectance in the bands in the visible. The difference in the red has been
31 discussed above (see Airmass composite). Regarding green, the 3.9 μ m radiance consists of a

1 solar and a thermal component during daytime, while reflection at this wavelength is sensitive
2 to cloud phase and very sensitive to particle size (high reflection indicates small particles).
3 Consequently, by subtracting the 10.8 μ m channel, the resulting values indicate water or ice
4 clouds with small or large particles. The difference between NIR1.6 and VIS0.6 in blue
5 provides information about the phase of the particles as the absorption at 1.6 μ m is highest for
6 the ice than for the water particles. The Convective storm image illustrates deep convection,
7 strong updrafts with small ice particles, from orange to yellow colours depending on the
8 strength of the updraft, while pink colour depicts precipitating clouds. Blue shades illustrate
9 land and ocean.

10

11 **4 Case study results and analysis**

12 **4.1 The period from 19 to 21 February 2013**

13 The Airmass and Convective storm composites were produced for four consecutive days 19,
14 20, 21, 22 February 2013, i.e. at a time period when a low pressure system was developed
15 over northwest Africa, moved eastward towards Greece causing instability and convection
16 over the regions which lie along the trajectory of the system.

17 During February 19, sinking dry air which could be of stratospheric origin was detected over
18 the western part of Europe, specifically from Great Britain to northwest Africa as it can be
19 seen from the reddish colour in the Airmass image at 12:00 UTC (Figure 5a). At the same
20 time, the 1 PVU level (Figure 5a) over western Europe is at 600hpa, which implies that
21 stratospheric air has protruded to mid troposphere, as it has been detected for the same region
22 also from the Airmass image (Figure 5a).The stratospheric intrusion is connected with high
23 potential vorticity values which in turn are related to cyclogenesis. Indeed, on February 20 at
24 00:00 UTC (Fig. 5b) a depression was formed over the northwest Africa, while at 12:00 UTC
25 (Fig. 5c) the depression was further developed. The Airmass image (Fig. 5c) depicts clearly
26 (with blue and green colours) the different air masses associated to the depression; the image
27 thus depicts clearly the cold and warm sectors respectively. In addition, due to the satisfactory
28 depiction of the cloud structure, the cold and warm fronts can be identified in the Airmass
29 image (Fig. 5c) through the developed clouds within the depression.

30 The sequence of the Airmass images (Fig. 5c - f) concerning the aforementioned days shows
31 the trajectory of the depression. According to the trajectory, the depression followed a zonal

1 track from the west towards the east. The depression moved along the African coast,
2 beginning from northwest Africa on February 20 at 12:00 UTC (Fig. 5c), passing over Sicily
3 on February 21 at 12:00 UTC (Fig. 5d, 5e) and located over south Greece on the February 22
4 at 00:00 UTC (Fig. 5f). This is a typical trajectory (easterly track) of African depressions in
5 February that differs from the respective trajectory in December and January. The latter has a
6 north component resulting in a northeast movement of the depression, thus affecting western
7 Mediterranean (Alpert et al., 1990).

8 Synoptic analysis for these days is presented on Fig. 6. Subsequent to the aforementioned PV
9 anomaly, a depression was developed on February 20 at 00:00 UTC, located over northwest
10 Africa with 1001hPa centre pressure (Fig. 6a), accompanied by a cut-off low in the upper
11 troposphere (Fig. 6b). Furthermore, on February 22, the warm sector of the depression is
12 located over Greece (Fig. 6c), while its centre lies easterly. The 500hpa height analysis (Fig.
13 6d) shows an extended trough located over central Europe and a disturbance connected with
14 the surface depression located over the Ionian Sea. It should be mentioned that the
15 aforementioned synoptic situation is similar to an examined one by Feidas et al. (2004) which
16 was classified as a west Depressional Weather Type in the classification of cold period
17 weather types in Greece. It is found that this type is related with convective activity and
18 atmospheric instability.

19 The passage of the depression over south Italy and Greece caused instability and resulted in
20 the development of convective cells over Sicily and Attica respectively. The Convective
21 storm images, as presented in sequence every fifteen minutes (Fig. 7), contribute to the
22 recognition, the diagnosis and the monitoring of the storm cells and their evolution to MCSs.

23 On February 21 after 12:57 UTC, the Convective image (Fig. 7a-7e) detects convective cells
24 (circular shape with orange to yellow colours) over Sicily. Subsequently, after 14:12 UTC the
25 merging of the storm cells which have evolved in MCSs is clearly observed (Fig. 7f). Both
26 MCSs continue to be yellow and to grow in size (Fig 7g-7i) indicating deep convection
27 without reaching yet the mature stages of their lifecycle. Furthermore, after 15:12 UTC (Fig.
28 7j-7l) the convective cells appear in pink signifying the weakening of the updraft or the
29 weakness of the Convective storm composite to provide reliable information due to the solar
30 zenith angle that approaches high values at sunset.

31 During the night of February 22, convective cells were developed over Attica, while in the
32 morning hours, and due to merging of the storm cells, a large Mesoscale Convective System

1 (MCS) is recognized (orange colour) in the Convective storm image at 09:42 UTC (Fig. 8a).
2 The MCS continues to grow in size without further affecting Attica, as it moves toward
3 southeast, (Fig. 9b-9f) while at 11:12 UTC (Fig. 8g) new cells develop (bright yellow colour)
4 within the southeast part of the MCS, highlighting the supply of the MCS with warm and
5 moist air from the southeast, a fact which indicates that the MCS has not yet reached the stage
6 of dissipation (Fig.8h-8l). Furthermore, convective activity is observed near the MCS for the
7 entire duration of its evolution. Consequently, the application of the Convective composite to
8 the above weather event shows its usefulness for the monitoring analysis of the evolution of a
9 MCS and thus demonstrates its capacity to support nowcasting.

10 **4.2 22 February 2013**

11 During the night of February 22 a series of extreme weather events occurred over Attica and
12 were related to the development of storm cells. At 00:00 UTC the warm sector of the low
13 pressure system was located over Greece (Fig. 6c). The south surface wind was supplying
14 Attica with warm and moist air, while at 850 hPa the same region was characterized by warm
15 advection and southeasterly winds. The passing of the cold front coupled with the
16 aforementioned situation led to the development of deep convection over Attica after 01:57
17 UTC. It should be mentioned that the total amount of precipitation for the eight hours period
18 (02:00 to 10:00 UTC) for all stations within Attica (Fig. 9), reflects the severity of the events.
19 For instance, Zografou station recorded 103mm, while the mean monthly precipitation for
20 February in Attica is 55-65 mm.

21 The use of Airmass composite (Fig. 10a,b,c,d) in conjunction with precipitation data every
22 ten minutes (Fig. 11) at the three stations that are located at the west, at the centre and at the
23 east of Attica, respectively, demonstrates the usefulness of this composite in nowcasting.

24 The first storm cell that was developed due to synoptic factors, is depicted in Airmass
25 composite at 01:57 UTC (Fig. 10a), i.e. forty to fifty minutes before the extreme weather
26 event's first maximum (Fig. 11). Subsequently, this storm cell evolved in a backward MCS
27 and the cold air as trapped in the Athens basin from the first MCS, and combined with the
28 south winds, established the conditions for further MCS development.

29 The second and the third storm cells are depicted at 02:57 UTC (Fig. 10b) and at 05:40 UTC
30 (Fig. 10c), respectively. These MCSs were depicted more than one hour earlier of the event,
31 third and fourth maxima (Fig. 11) and eventually both of them evolved in forward MCSs.

1 Finally, the merging of the two MCSs is depicted at 06:57 UTC (Fig. 11d), twenty minutes
2 earlier of the event and resulted in the reinforcement of the extreme event for the fourth time
3 (Fig. 11).

4 Finally, the differences in the precipitation distribution between the three stations are
5 attributed to the change in direction of the mean wind in 850 – 300 hPa layer. After their
6 development within the MCS, the cells moved downwind with the mean wind affecting
7 different regions depending on the wind direction. Particularly, the cells of the first MCS
8 moved towards north, as the mean wind was south, affecting Ano Liosia and Galatsi stations.
9 Subsequently the south mean wind started to have a west component and carried the cells
10 towards northeast of Attica (Zografou station).

11

12 **5 Conclusion**

13 This research study aims at demonstrating the potential for the early detection and adequate
14 monitoring of storm cells associated to natural hazards. The developed methodology was
15 applied for a four day long case study in February 2013, when a low pressure system
16 developed over Africa and moved north eastward towards Greece causing instability along its
17 trajectory. The methodology focuses in particular to the series of extreme weather events that
18 occurred on the 22nd of February 2013 for a period of seven hours over Attica.

19 The procedure developed for the production of the composites (Airmass and Convective
20 storm), provides all products at fifteen minutes interval, a fact which improves the capacity to
21 operationally observe the evolution of a MCS as well as it merging to other MCSs. The
22 application of these composites shows that the Airmass composite depicts well the synoptic
23 situation and detects the PV anomaly prior to the depression development. The extended use
24 of this composite to storm cell detection, allowed the detection of three MCS that produced
25 four precipitation maxima. Comparing the distribution of the precipitation amount with the
26 produced images, it is deduced that the methodology enables the detection of three storm cells
27 at least one hour earlier from the events in all stations and twenty minutes earlier from the
28 merging of the cells. Furthermore, the application of the Convective storm, when available, to
29 the above weather event shows its usefulness for the monitoring of the evolution of MCS. In
30 particular, the use of the Convective storm allowed the depiction of deep convection over
31 Sicily and Attica, as well as the identification of the MCS region where the new cells
32 developed.

1 In conclusion, despite the limitations (for instance the lack of the Convective Storm
2 composite during night time), the performed analysis demonstrate the potential of earth
3 observation, once combined with ground based data, for the recognition, the analysis and the
4 monitoring of the MCSs associated with natural hazards. Taken the potential impacts of
5 natural hazards to human well being, a critical prerequisite for the monitoring of the MCSs is
6 the rapid re-examination of the prevailing meteorological and storm cell conditions; such
7 prerequisite is satisfied by developing the Air Mass and Convective storm composites at
8 fifteen minutes intervals. Finally further work is needed, for instance the use of additional
9 composites to compensate for the lack of the Convective storm one at night, so as to improve
10 the analysis and support nowcasting techniques.

11

12

1 **References**

- 2 Alpert, P., Neeman, B. U., and Shay-el, Y.: Intermonthly Variability of Cyclone Tracks in the
3 Mediterranean. *J Climate* 3, 1474-1478, 1990.
- 4 Anderson, C. J., and Arritt, R. W.: Mesoscale convective complexes and persistent elongated
5 convective systems over the United States during 1992 and 1993. *Mon Weather Rev*, 126,
6 578–599, 1998.
- 7 Campins, J., Genovés, A., Jansà, A., Guijarro, A. J., and Ramis, C.: A catalogue and a
8 classification of surface cyclones for the western Mediterranean. *Int J Climatol*, 20, 969-984,
9 2000.
- 10 Cartalis, C., Chrysoulakis, N., Feidas, H., and Pitsitakis, N.: Categorization of cold period
11 weather types in Greece on the basis of the photointerpretation of NOAA/AVHRR imagery.
12 *Int J Remote Sens*, 25, 2951-2977, 2004.
- 13 Casanova, C., Romo, A., Hernández E., and Casanova, L. J.: Operational cloud classification
14 for the Iberian Peninsula using Meteosat Second Generation and AQUA-AIRS image fusion.
15 *Int J Remote Sens*, 31, 93-115, 2010.
- 16 Cotton, W. R., and Anthes, R. A.: *Storm and Cloud Dynamics*. San Diego: Academic Press,
17 1989.
- 18 Davis, C., and Emanuel, K.: Potential Vorticity Diagnostics of Cyclogenesis. *Mon Weather*
19 *Rev*, 119, 1929-1953, 1991.
- 20 Feidas, H., Cartalis, C., and Cracknell, A.: Use of Meteosat imagery to define clouds linked
21 with floods in Greece. *Int J Remote Sens*, 21, 1047-1072, 2000.
- 22 Feidas, H., and Cartalis, C.: Monitoring Mesoscale Convective Cloud Systems Associated
23 with Heavy Storms Using Meteosat Imagery. *J Appl Meteorol*, 40, 491-512, 2001.
- 24 Feidas, H., and Cartalis, C.: Application of an automated cloud-tracking algorithm on satellite
25 imagery and monitoring small mesoscale convective cloud systems. *Int J Remote Sens*, 26,
26 1677-1698, 2005.
- 27 Feidas, H.: Study of a Mesoscale Convective Complex Over Balkans with Meteosat Data.
28 *Advances in Meteorology, Climatology and Atmospheric Physics Springer Atmospheric*
29 *Sciences*, pp. 79-85, 2012.

1 Gallino, S., and Turato, B.: An operational approach to the nowcasting of an intense
2 thunderstorm over Liguria. *Adv Geosci*, 7, 395-400, 2006.

3 Giannakos, A., and Feidas, H.: Classification of convective and stratiform rain based on the
4 spectral and textural features of Meteosat Second Generation infrared data. *Theor App*
5 *Climatol*, 113, 495-510, 2013.

6 Glickman, T.: Glossary of meteorology. 2d ed. American Meteorological Society, pp. 855,
7 2000.

8 Hoskins, J. B., McIntyre, E. M., and Robertson, W. A.: On the use and significance of
9 isentropic potential vorticity maps. *Q J R Meteorol Soc*, 111, 877-946, 1985.

10 Houze, R.: Mesoscale Convective Systems. *Reviews of Geophysics* 42,
11 10.1029/2004RG000150, pp. 43, 2004.

12 Kerkmann J., Rosenfeld, D., Bridge, G., and Roesli, H.: RGB applications patr04, RGB
13 composites with channels 1-11 and their interpretation. Available online at
14 <http://www.eumetrain.org/IntGuide/>, 2006.

15 Kolios, S., and Feidas, H.: A warm season climatology of mesoscale convective systems in the
16 Mediterranean basin using satellite data. *Theor App Climatol*, 102, 29-42, 2010.

17 Laing, A. G., and Fritsch, J. M.: The large-scale environments of the global populations of
18 mesoscale convective complexes. *Mon Weather Rev*, 128, 2756–2776, 2000.

19 Maddox, R. A.: Large-scale meteorological conditions associated with midlatitude, mesoscale
20 convective complexes. *Mon Weather Rev*, 111, 126–140, 1983.

21 Melani, S., Pasi, F., Gozzini, B., and Ortolani, A.: A four year (2007-2010) analysis of long-
22 lasting deep convective systems in the Mediterranean basin. *Atmos. Res*, 123, 151-166, 2013.

23 Michel, Y., and Bouttier, F.: Automated tracking of dry intrusions on satellite water vapour
24 imagery and model output. *Q J R Meteorol Soc*, 132, 2257-2276, 2006.

25 Negri, G. R., Machado, T. A. L., and Borde, R.: Inner convective system cloud-top wind
26 estimation using multichannel infrared satellite images. *Int J Remote Sens*, 35, 651-670, 2014.

27 Pajek, M., Iwanski, R., Konig, M., and Struzik, P.: Extreme Convective Cases - The use of
28 Satellite Products for Storm Nowcasting and Monitoring, EUMETSAT Conference Report,
29 Darmstadt, Germany, 2007.

- 1 Pankiewicz, S. G.: Neural network classification of convective airmasses for flood forecasting
2 system. *Int J Remote Sens*, 18, 887-898, 1997.
- 3 Petterssen, S.: *Weather Analysis and Forecasting*, vol. I. MacGraw-Hill: New York; 428 pp,
4 1956.
- 5 Putsay, M., and Szenyan, I., Simon, A.: Case study of Mesoscale Convective Systems over
6 Hungary on 29 June 2006 with satellite, radar and lightning data. *Atmos. Res*, 93, 82-92,
7 2009.
- 8 Radinovic, D.: *Mediterranean cyclones and their influence on the weather and the climate*.
9 WMO, PSMP Rep. Ser. num 24, 1987.
- 10 Vila, A. D., and Machado, T. A. L.: Shape and radiative properties of convective systems
11 observed from infrared satellite images. *Int J Remote Sens*, 25, 4441-4456, 2004.
- 12 Ziv, B., Saaroni, H., Romem, M., Heifetz, E., Harnik, N., and Baharad, A.: Analysis of
13 conveyor belts in winter Mediterranean cyclones. *Theor Appl Climatol*, 99, 441-455, 2010.
- 14

1 Table 1 Characteristics of the eight MSG channels used for the composites production.

Channel No.	Spectral Band (μm)	Range of spectral band (μm)	Main observational application
01	VIS0.6	0.56-0.71	Surface, clouds, wind fields
03	NIR1.6	1.50-1.78	Surface, cloud phase
04	IR3.9	3.48-4.36	Surface, clouds, wind fields
05	WV6.2	5.35-7.15	Water vapor, high level clouds, atmospheric instability
06	WV7.3	6.85-7.85	Water vapor, atmospheric instability
08	IR9.7	9.38-9.94	Ozone
09	IR10.8	9.80-11.80	Surface, clouds, wind fields, atmospheric instability
11	IR13.4	12.40-14.40	Cirrus cloud height

2



1

2

3 Figure 1. Area of study in Meteosat projection

4

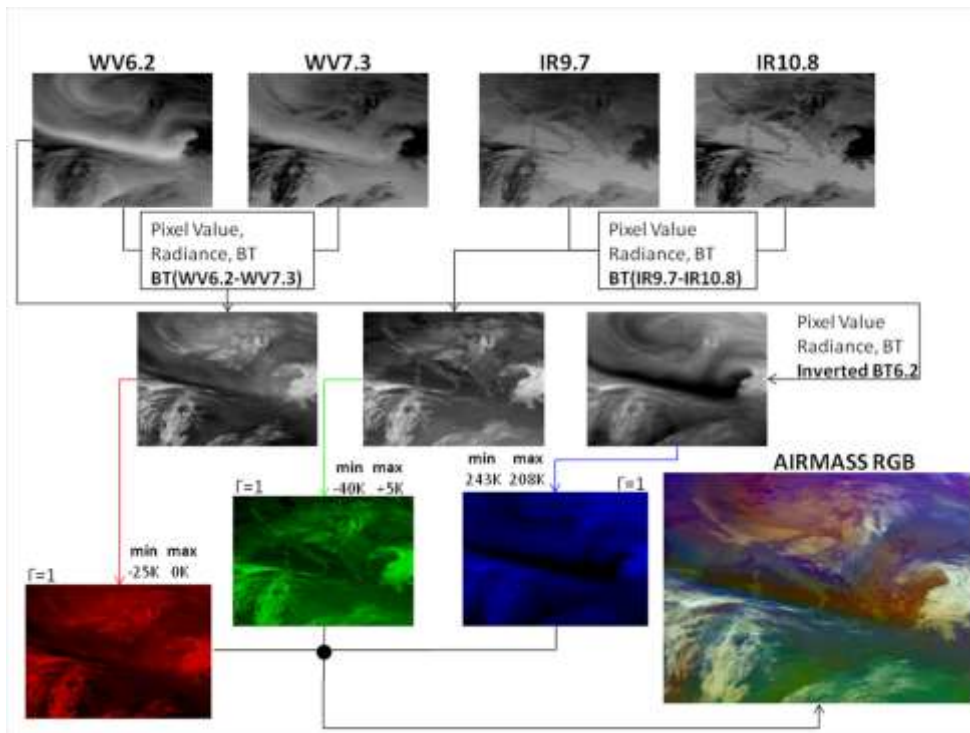


1

2

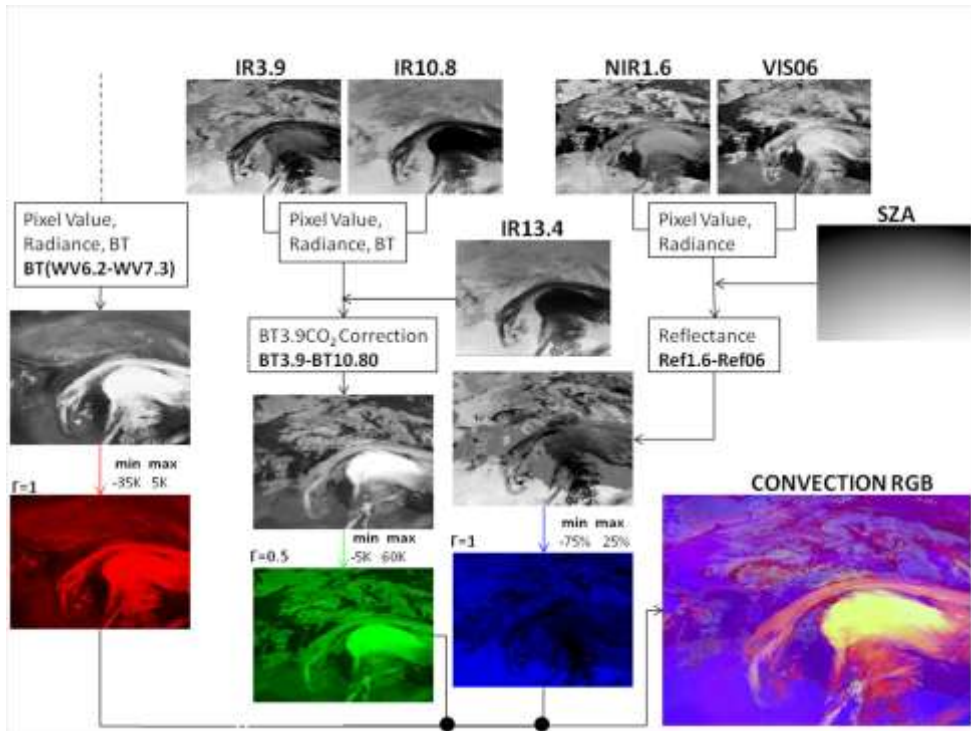
3 Figure 2. Attica region and the location of the eight meteorological stations.

4



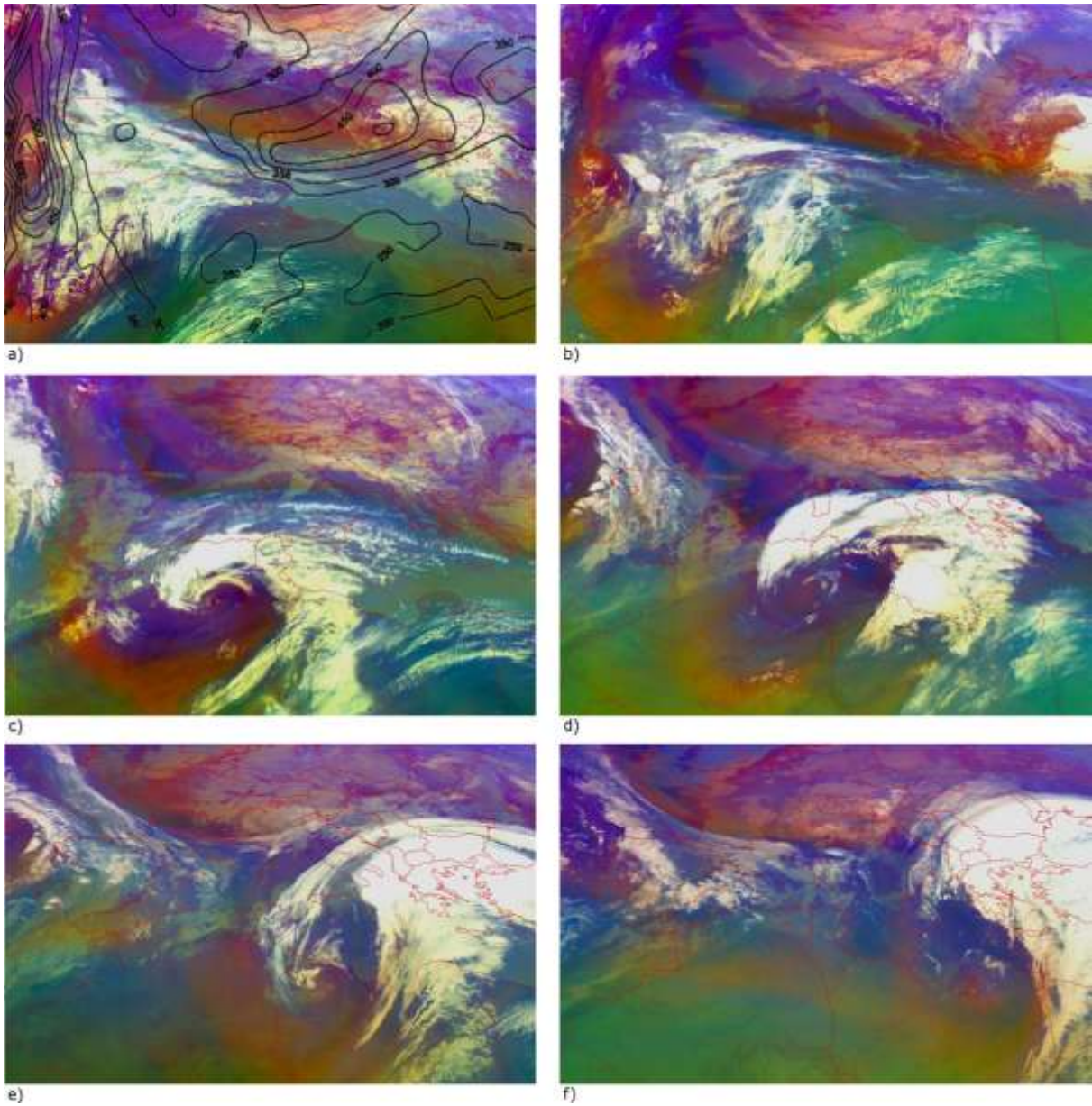
1
2
3
4

Figure 3. Flow chart of the procedure followed for the Airmass composite production.

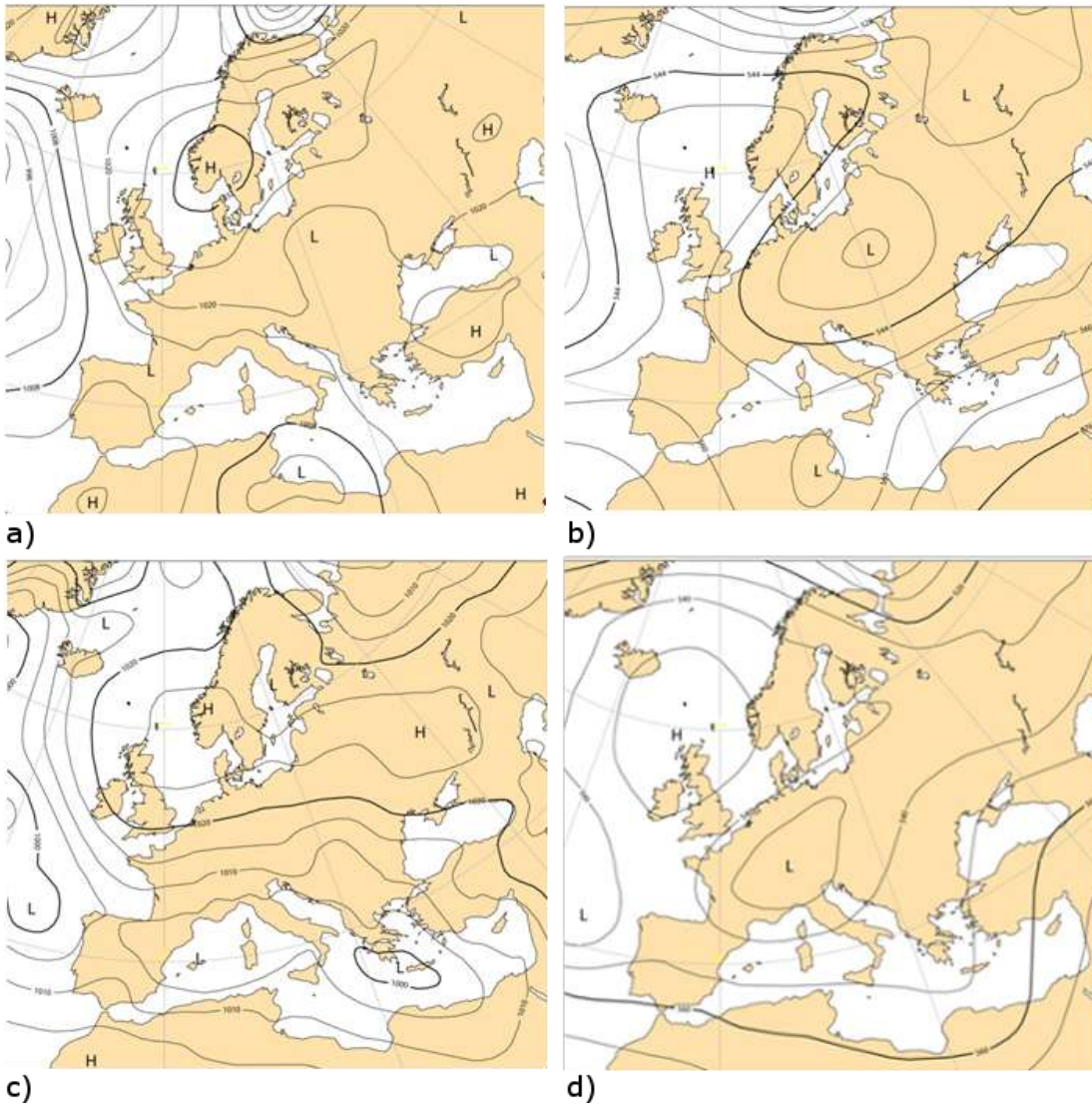


1
2
3
4
5
6

Figure 4. Flow chart of the procedure followed for the Convection storm composite production.

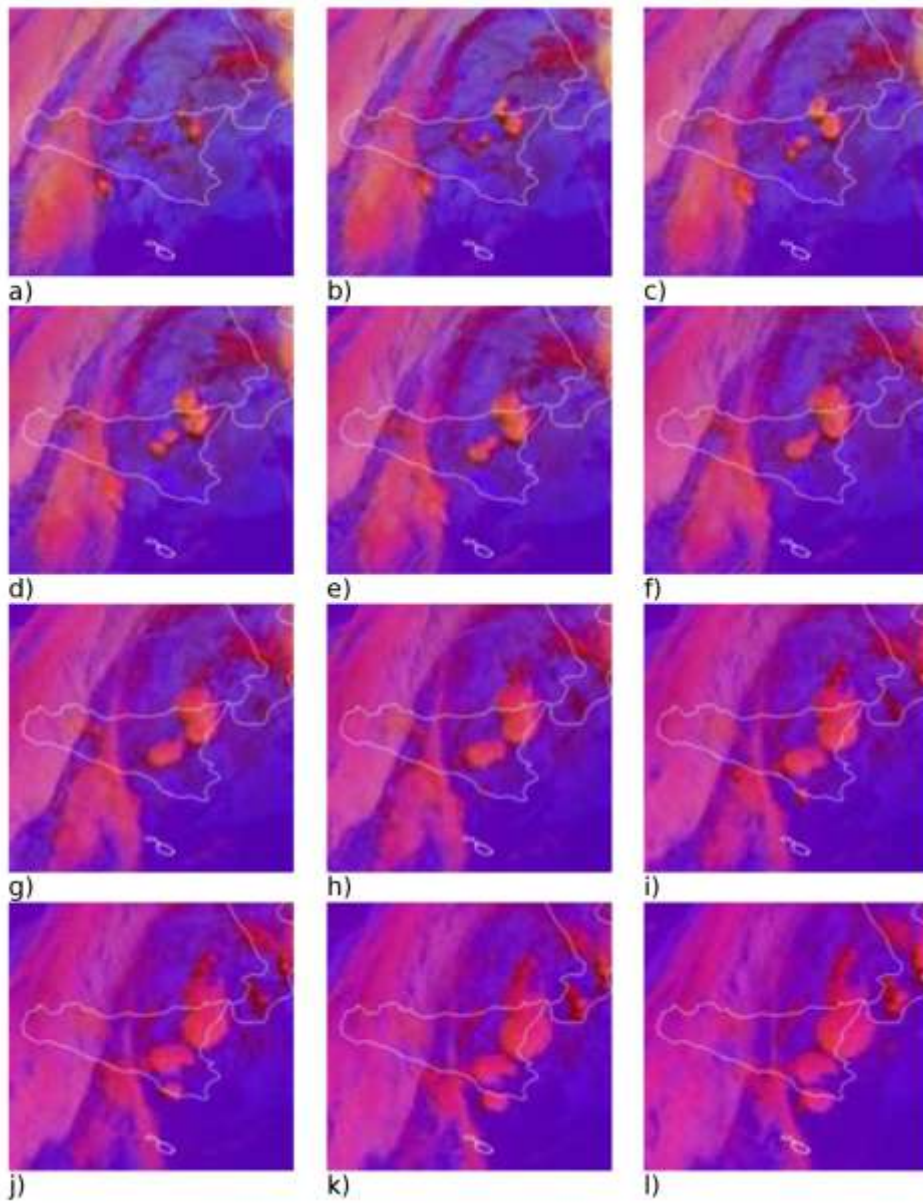


1
 2 Figure 5. Airmass composite images on a) February 19 at 12:00 UTC overlaid with the 1
 3 PVU level, b) February 20 at 00:00 UTC, c) February 20 at 12:00UTC, d) February 21 at
 4 00:00UTC, e) February 21 at 12:00UTC and f) February 22 at 00:00UTC
 5



1 c) d)
 2 Figure 6. Synoptic charts for different atmospheric levels on February 20 at 00:00 UTC a)
 3 surface pressure chart, b) 500hPa geopotential height and on 22 February at 00:00 UTC c)
 4 surface pressure chart and d) 500hPa geopotential height

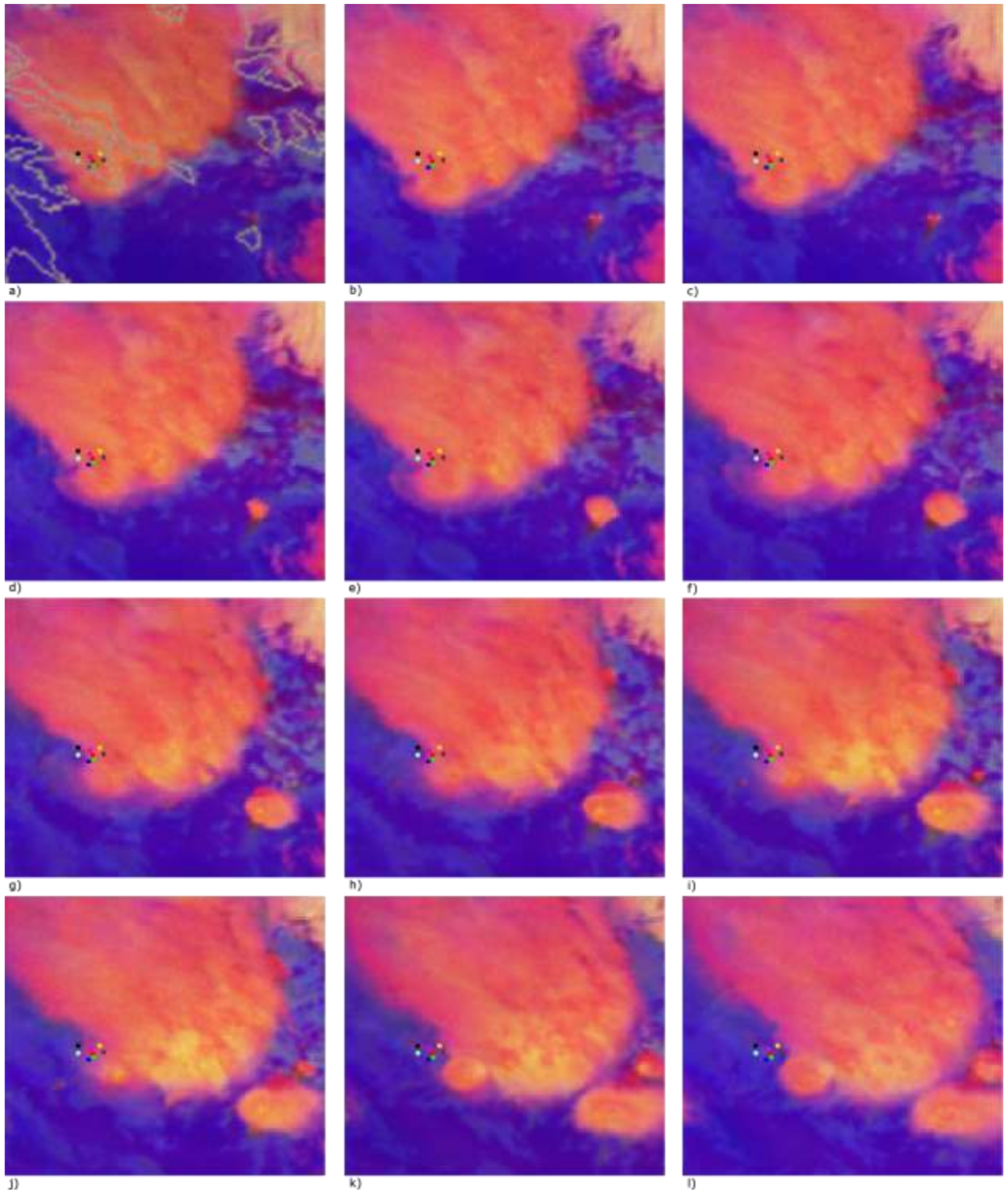
5



1

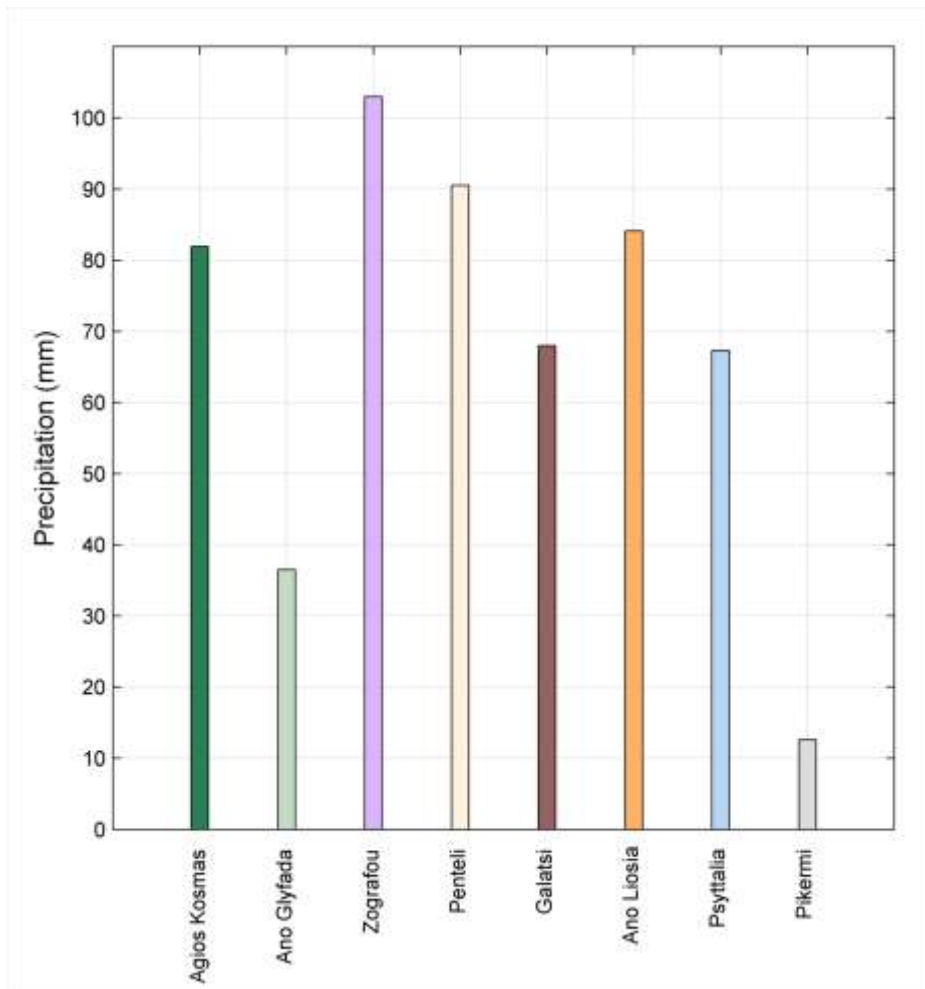
2 Figure 7. Convective storm images (focused on Sicily) on February 21 every fifteen minutes
3 from a) 12:57 UTC to l) 15:42 UTC

4



1
2
3
4
5
6

Figure 8. Convective storm composite images (focused on Attica) on February 22 every fifteen minutes from a) 09:42 UTC to l) 12:27 UTC. Coloured circles indicate the weather stations within Athens basin (black: Ano Liosia, purple: Galatsi, red: Zografou, blue: Agios Kosmas, green: Ano Glyfada, yellow: Penteli, grey: Pikermi, light blue: Psytalia)

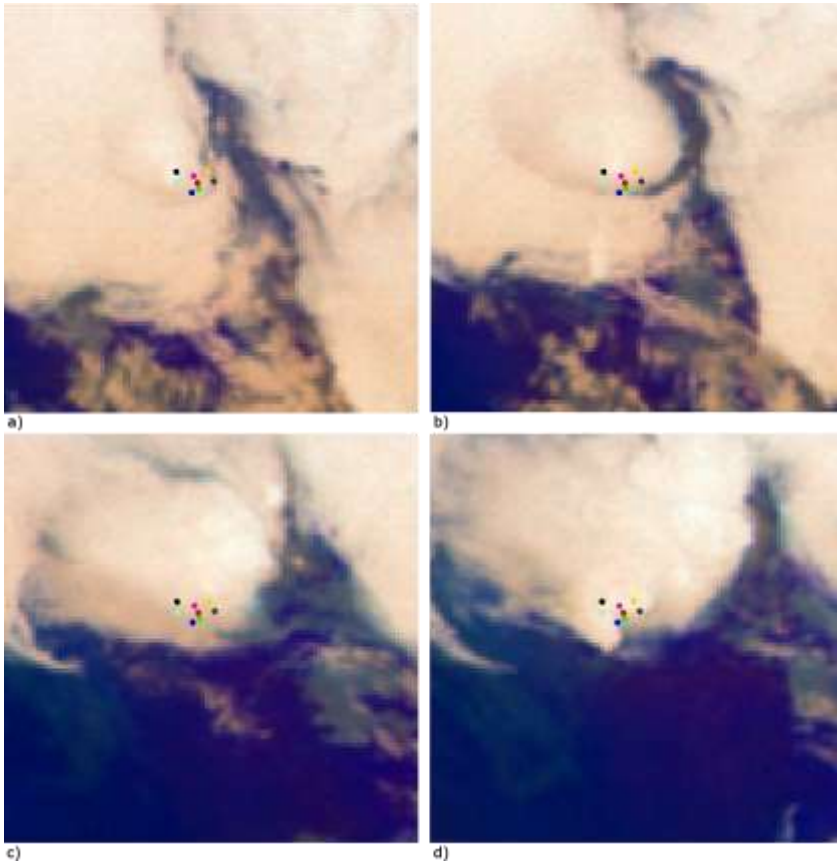


1

2

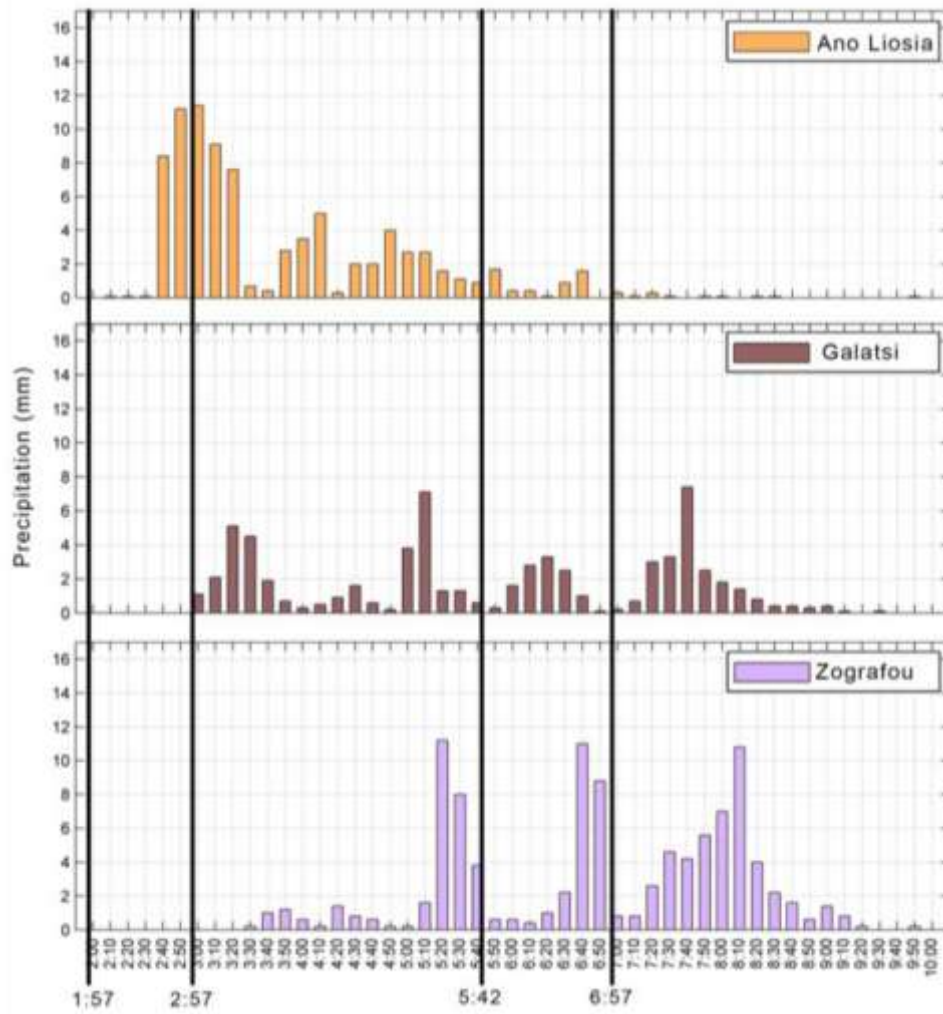
3 Figure 9. Total amount of precipitation for the eight hours period (02:00 to 10:00 UTC) for all
4 stations within Attica

5



1
2
3
4
5
6
7

Figure 10. Airmass composite (focused on Attica) on February 22 at a) 01:57 UTC, b) 02:57 UTC, c) 05:40 UTC and d) 06:57 UTC. Coloured circles indicate the weather stations within Athens basin (black: Ano Liosia, purple: Galatsi, red: Zografou, blue: Agios Kosmas, green: Ano Glyfada, yellow: Penteli, grey: Pikermi, light blue: Psyttalia)



1

2

3 Figure 11. Precipitation data every ten minutes at three stations Ano Liosia, Galatsi and

4 Zografou